Enhanced mechanical properties of boron nitride nanosheets/copper composites with a bioinspired laminated structure

Yun Wang, Can Huang, Ruitao Li, Hong Liu, Zhenying Xu, Chao Yu & Hua Li

Check for updates

Enhanced mechanical properties of boron nitride nanosheets/copper composites with a bioinspired laminated structure

Yun Wang[a], Can Huang[a], Ruitao Li[a], Hong Liu[a], Zhenying Xu[a], Chao Yu[a] and Hua Li [b]

[a]School of Mechanical Engineering, Jiangsu University, Zhenjiang,Jiangsu Province,China; [b]Key Laboratory of Marine Materials and Related Technologies, Zhejiang Key Laboratory of Marine Materials and Protective Technologies, Ningbo Institute of Materials Technology and Engineering, Chinese Academy of Sciences, Ningbo, Zhejiang Province, China

ABSTRACT

Poor mechanical properties of copper (Cu) hinder its applications as structural materials. Developing bioinspired-laminated structure is among the most promising strategies for obtaining modern structural materials with excellent combination mechanical properties. To explore the possibility of enhancing mechanical properties of Cu, herein, we fabricated boron nitride nanosheets/copper (BNNSs/Cu) composites with a bioinspired laminated structure, achieved by ball milling and spark plasma sintering (SPS). Their mechanical properties were investigated. The results indicate that their tensile strength and toughness are both larger than those of pure Cu: the addition of 0.3 vol% of BNNSs improves the tensile strength from 187 MPa to 216 MPa and the elongation from 41% to 56%, respectively. The enhancement of ductility is due to the unique lamellar distribution of BNNSs in composites, which resulted in retarding cracks propagation; the strengthening effect of BNNSs is determined by the moderate interfacial bonding strength and possible agglomeration of BNNSs.
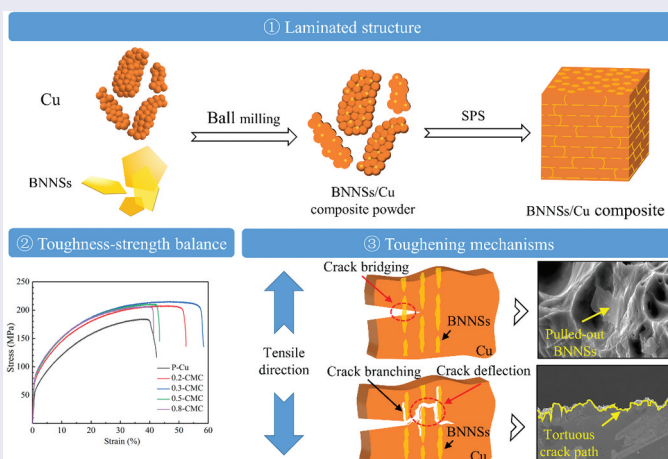
CONTACT Ruitao Li ✉ RLI3@e.ntu.edu.sg 🏫 School of Mechanical Engineering, Jiangsu University, Zhenjiang, Jiangsu Province, China;

1. Introduction

Metal matrix composites (MMCs) are extensively used for structural materials due to their superb combination properties. As a commonly used matrix materials, copper (Cu) has many outstanding properties such as excellent ductility, high electric conductivity and superb thermal conductivity [1,2]. But its low strength is the main disadvantage [3]. Therefore, Cu-based matrix composites have been widely investigated for their excellent mechanical properties [4–7]. However, most Cu-based matrix composites often pursuit high strength while compromising their toughness [8,9], which extremely limits their engineering applications in the fields of aerospace, automobile and military industries [10]. Therefore, it is vital to improve strength while retaining excellent toughness.

Hundreds of million years of evolution make most living things have an extraordinary combination of mechanical properties, including high strength and remarkable toughness [11,12], which originate from their unique microstructure. For example, nacre is a natural composite consisting of brittle layers of mineral and a small fraction of organic constituents [13]. But it has not only high strength but also splendid toughness [14–16], because of its laminated structure – which takes effect in hindering crack formation and propagation [17–19]. Such bioinspired laminated structure provides a potential solution to dealing with the strength-toughness conflict in Cu-based matrix composites [20]. Until now, one-dimensional (1D) reinforcements/metal composites with laminated structure have been successfully fabricated with balanced strength and toughness [21–26]. For example, the study by Song et al. [27] showed that the strength and elongation of the laminated CNTs/Mg composites were increased by 52% and 59%, respectively. However, due to the geometry compatibility with the planar laminated structure, two-dimensional (2D) materials are considered as exceptional reinforcement candidate for the laminated composites [28]. Boron nitride nanosheets (BNNSs), which consist of alternating boron (B) and nitrogen (N) atoms in a hexagonal lattice, possess superior mechanical and functional properties such as high tensile strength (30 GPa) [29,30], high Young's modulus (850 GPa) [31,32], high thermal conductivity (1700–2000 W/m·K) [33], high thermal stability (up to 900°C) [34], high chemically stable [35], low dielectric constant (3–5) [36] and excellent lubrication ability [37]. Thus, they are expected to be an ideal reinforcements of laminated composites. Recently, Yoo et al. [38] fabricated BNNSs/Cu composites with random distribution of BNNSs and the tensile strength of composites was increased by 40%, indicating the potential strengthening effect of BNNSs in Cu-based matrix composites. However, the strength-toughness conflict issue is still unsolved – the elongation was decreased seriously (about 27%). Thus, it is hopeful to develop Cu-based matrix composites with well-balanced strength and toughness by the combination of the toughening effect of laminated structure and strengthening effect of BNNSs.

In this study, ball milling and spark plasma sintering (SPS) were used to fabricate BNNSs/Cu composites with bioinspired laminated structure. The effect of BNNSs on mechanical properties in BNNSs/Cu composites was investigated. The microstructures, strengthening and toughening mechanisms of BNNSs/Cu composites were discussed.
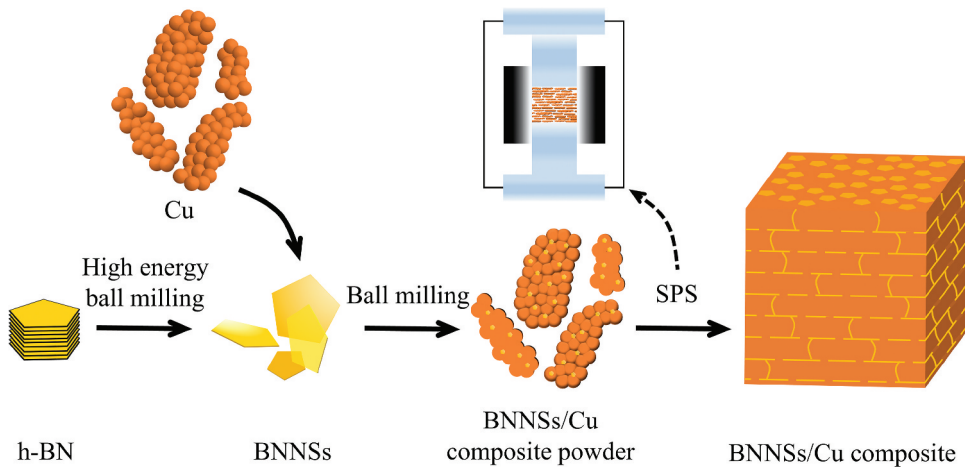
Figure 1. Schematic of fabrication process of BNNSs/Cu composite.

2. Experimental

2.1 Materials

Commercial hexagonal boron nitride (h-BN) particles were purchased from Beijing Xing Rong Yuan Technology Co., Ltd. Electrolytic copper powder (Cu, 99.9% purity) with a size of 20 ~ 40 μm were provided by Jiangsu Men Da New Materials Technology Co., Ltd.

2.2 Preparation of the BNNSs/Cu composites

The schematic drawing of fabrication process of BNNSs/Cu composites is illustrated in Figure 1. The BNNSs were exfoliated from h-BN via high-energy ball milling (HEBM, YXQM-2 L, Changsha Miqi Instrument Equipment Co., Ltd.). The pristine h-BN particles were milled with stainless steel balls of three different sizes (diameter = 5, 10 and 15 mm) of 5:3:2 at the rotational speed of 700 rpm for 40 min using alcohol as the dispersing agent. The ball-to-powder ratio was maintained at 40:1. The milling process was carried out under purity argon and at intervals of 2 min for 2 min of cooling. Then, the resulting solution was dried at 60°C for 24 h to let the alcohol evaporate.

The exfoliated BNNSs powder was mixed with Cu powder by ball milling at the rotational speed of 200 rpm for 30 min in stainless steel vials with stainless steel balls of 5 mm. The ball-to-powder ratio chosen was 20:1. The milling process was carried out also under purity argon and at intervals of 2 min for 2 min of cooling. Then the as-prepared BNNSs/Cu composite powder was consolidated by SPS (Labox-325, SINTER LAND INC.) at 850°C under a uniaxial pressure of 50 MPa for 10 min with a heating rate and cool rate of 100°C/min. For comparison, samples of pure Cu and composites with 0.2, 0.3, 0.5 and 0.8 vol% BNNSs were fabricated under the same condition, and they were labeled as P-Cu, 0.2-CMC, 0.3-CMC, 0.5-CMC and 0.8-CMC, respectively.

2.3 Characterization of the BNNSs/Cu composites

The theoretical densities of pure Cu and BNNSs were 8.9 and 2.25 g/cm^3, respectively. The density of the BNNSs/Cu composites was calculated by the Archimedes principle. The microstructure of starting powder and BNNSs/Cu composites was characterized using scanning electron microscopy (SEM, S3400, Hitachi), field-emission scanning electron microscopy (FE-SEM, JSM7800F, JEOL), transmission electron microscopy (TEM, Tecnai G2 F20, FEI) and Optical microscopy (OM, MR5000, Jueyu Technology).

2.4 Mechanical testing

Tensile testing experiments were conducted on a DDL100 electron universal testing machine with a crosshead speed of 1 mm/min at room temperature. For tensile testing, the obtained samples were cut to a dog-bone shape with a gauge length of 8 mm, a gauge width of 2.2 mm and a thickness of 1 mm, respectively. Three tensile specimens for each material were tested.

3. Results and discussion

3.1 Raw powders

The morphology of Cu particles and BNNSs are presented in Figure 2. Figure 2a indicates that the as-received Cu particles has the typical dendritical morphology. Figure 2b is the bright field TEM image of the BNNSs powder obtained after the mechanical exfoliation process. It can be seen that there are some wrinkles and folds on the surface of the BNNSs.

Figure 3 shows the morphology of BNNSs/Cu composite powder with 0.3 vol% and 0.8 vol% BNNSs. The shape of BNNSs/Cu composite powder changed in the ball milling process: most of them were flattened due to the impact of steel balls (Figure 3a and c). This made them be well aligned under the uniaxial pressure of SPS, in which benefits the formation of a laminated structure. In addition, BNNSs were homogeneously dispersed
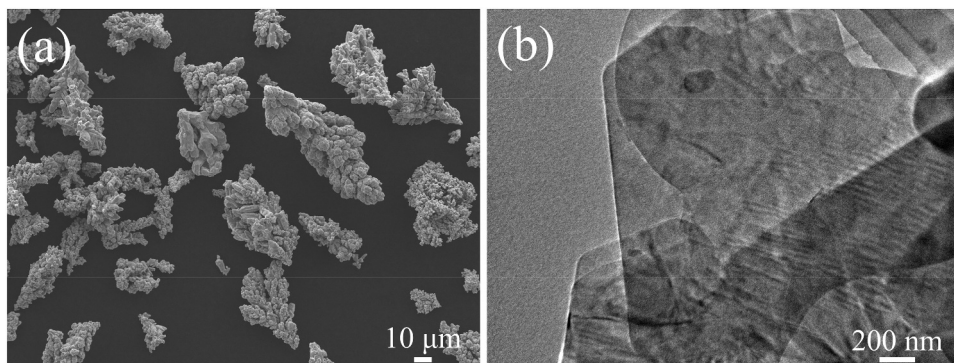

Figure 2. Characterizations of Cu particles and BNNSs powder. (a) SEM image of the as-received Cu particles; (b) TEM image of the BNNSs powder.
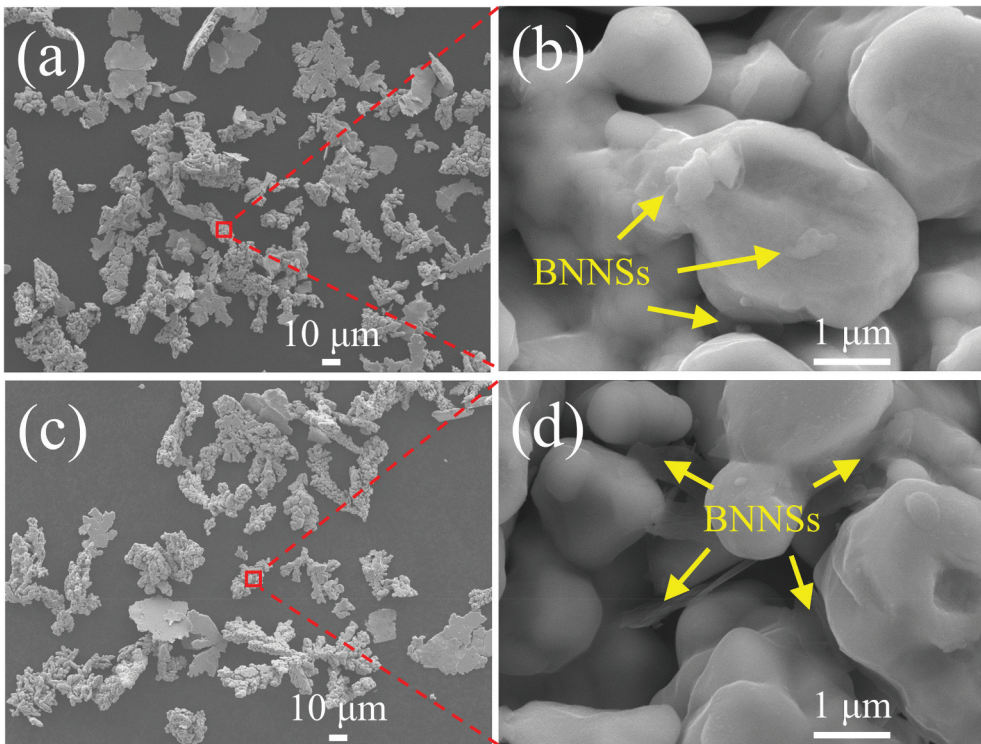
Figure 3. SEM images of the morphology of BNNSs/Cu composite powder with (a, b) 0.3 vol.%; (c, d) 0.8 vol.% BNNSs.

Table 1. Theoretical, experimental and relative densities along with porosity content of BNNSs/Cu composites.

Materials	Theoretical density (g/cm^3)	Experimental density (g/cm^3)	Relative density (%)	Porosity (%)
0.2-CMC	8.887	8.867 ± 0.01	99.77 ± 0.10	0.23 ± 0.10
0.3-CMC	8.880	8.853 ± 0.01	99.70 ± 0.10	0.30 ± 0.10
0.5-CMC	8.867	8.831 ± 0.01	99.60 ± 0.06	0.40 ± 0.06
0.8-CMC	8.848	8.810 ± 0.01	99.57 ± 0.06	0.43 ± 0.06

in Cu matrix during the mixture process of ball milling, when their content was 0.3 vol% (Figure 3b). However, Figure 3d shows excess BNNSs may result in the agglomeration of BNNSs, when their content reached 0.8 vol%.

3.2 Densities and microstructures of the composites

The theoretical, experimental and relative densities as well as porosity content of the BNNSs/Cu composites are shown in Table 1. As can be seen, the relative density of all samples are above 99%, indicating that near-full density materials were produced during SPS process. Therefore, the impact of porosity content on the mechanical properties of BNNSs/Cu composites can be negligible.
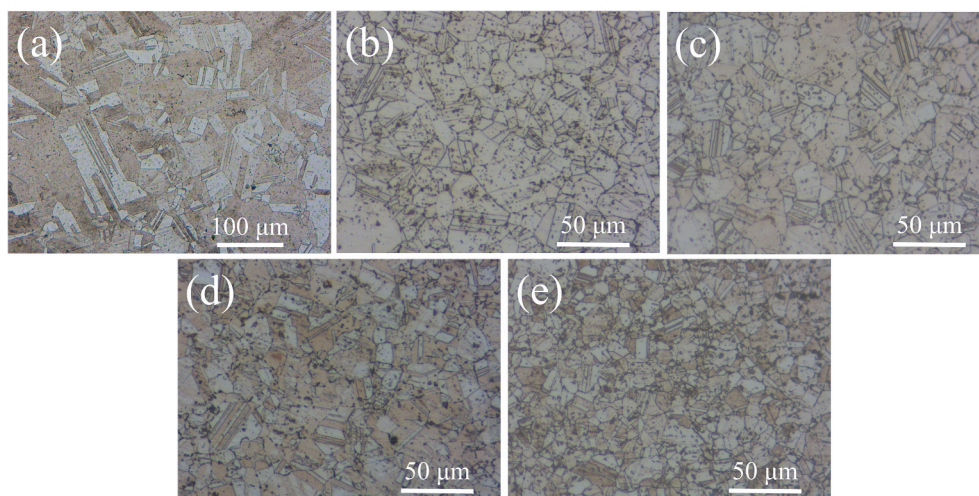
Figure 4. OM images of grain structure of P-Cu and BNNSs/Cu composites. (a) P-Cu; (b) 0.2-CMC; (c) 0.3-CMC; (d) 0.5-CMC; (e) 0.8-CMC.

Table 2. Average grain size of P-Cu and BNNSs/Cu composites.

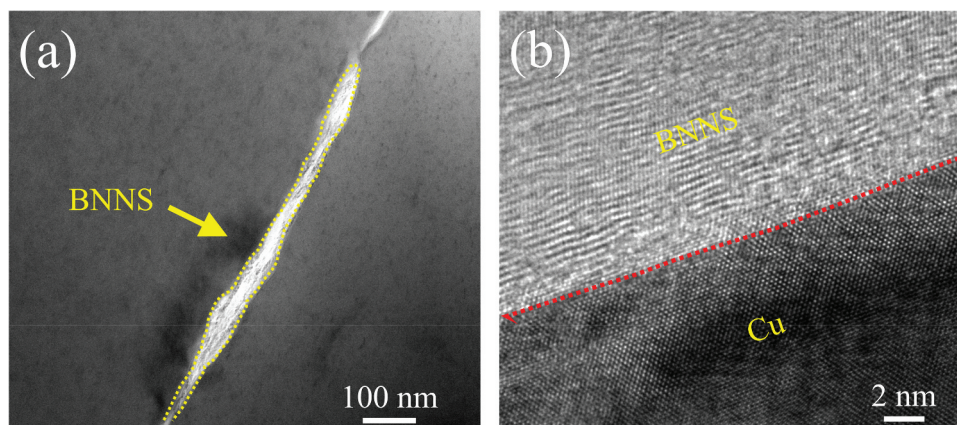| Materials	Average grain size (μm)
P-Cu	18.0 ± 0.4
0.2-CMC	8.2 ± 0.2
0.3-CMC	7.9 ± 0.1
0.5-CMC	7.2 ± 0.1
0.8-CMC	6.4 ± 0.3

Figure 5. (a) TEM characterization of the interfacial region; (b) HRTEM image of interface.

Figure 4 shows the OM images of grain structure of P-Cu and BNNSs/Cu composites with different BNNSs contents. The average grain size was estimated by a line intercept method. Detailed data are presented in Table 2. Clearly, the introduction of BNNSs can
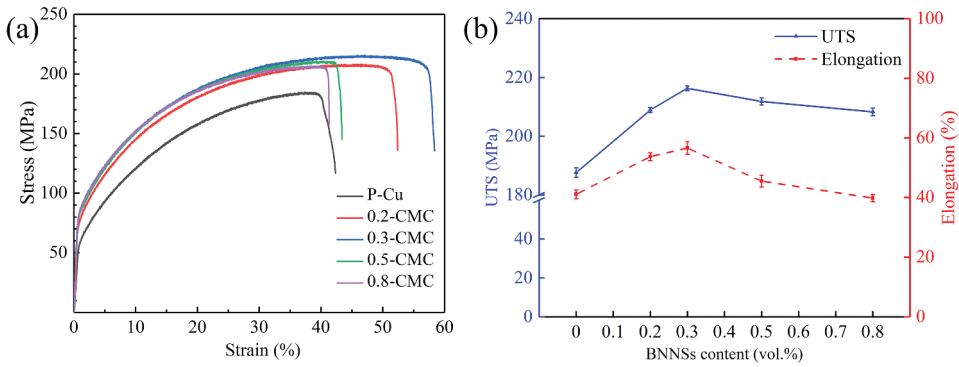
Figure 6. Tensile properties of P-Cu and BNNSs/Cu composites. (a) Stress-strain curves; (b) relationship of UTS and δ with different BNNSs contents.

Table 3. Tensile properties of P-Cu and BNNSs/Cu composites.

Materials	UTS (MPa)	Elongation (%)	WOF (MJ/m^3)
P-Cu	187 ± 2	41.1 ± 1.5	60.1 ± 1.5
0.2-CMC	208 ± 1	53.7 ± 1.3	94.9 ± 2.8
0.3-CMC	216 ± 1	56.6 ± 2.1	104.5 ± 4.0
0.5-CMC	211 ± 1	45.5 ± 2.0	79.5 ± 4.4
0.8-CMC	208 ± 1	39.8 ± 1.2	68.7 ± 1.7

refine the grains. With an increased BNNSs content, the average grain size of composites decreased.

Figure 5 provides the TEM characterization of the interfacial region. No visible voids and cracks were present in this region, indicating that BNNSs and Cu matrix were well bonded. A tortuous BNNSs/Cu interface was formed due to the rough surface of BNNSs (Figure 5a). Such characteristic can improve the toughness of composites by deflecting cracks when subjected to stress. Figure 5b shows the HRTEM image of interfacial microstructure. No impurities or transitional layer could be observed. Actually, such interface can be categorized into the diffusional interface, as the diffusion of B into Cu can be expected in the sintering process [39,40]. The bonding strength of such interface is moderate [41,42]. Its influences on the properties of the composites will be discussed in the Discussion section.

3.3 Mechanical properties

Tensile properties of P-Cu and BNNSs/Cu composites with different BNNSs contents are presented in Figure 6. Figure 6a exhibits the stress-strain curves of BNNSs/Cu composites. Figure 6b shows the relationship of ultimate tensile strength (UTS) and elongation (δ) of BNNSs/Cu composites with different BNNSs contents. Detailed data are presented in Table 3. Obviously, the tensile properties of BNNSs/Cu composites were improved significantly. With the increasing of BNNSs content, the UTS and δ of the composites initial increased and then decreased, with 0.3 vol% being a turning point. The UTS of 216 MPa at the BNNSs content of 0.3 vol% was increased by 15.3% compared to that of P-Cu (187 MPa). As for the ductility, the largest δ of 56.6% was also obtained when the BNNSs
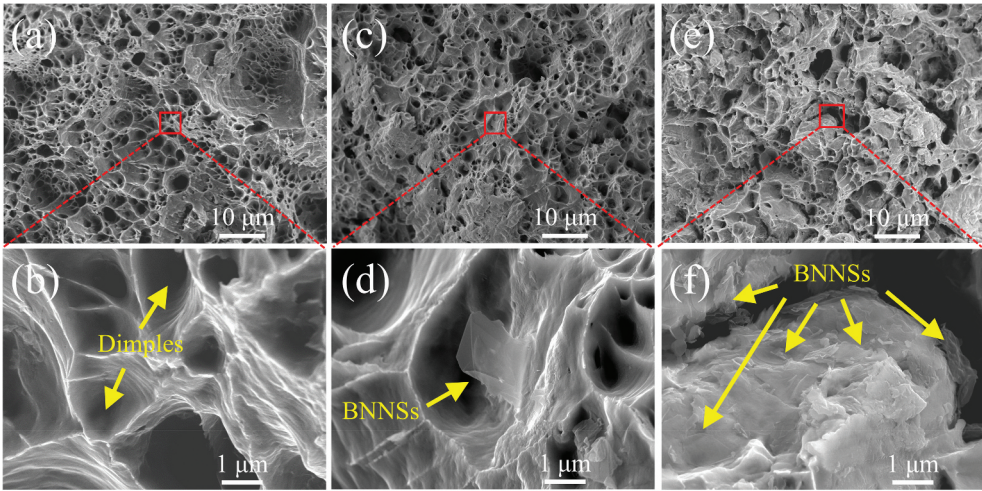
Figure 7. SEM images of the fracture surfaces of (a, b) P-Cu; (c, d) 0.3-CMC; (e, f) 0.8-CMC.
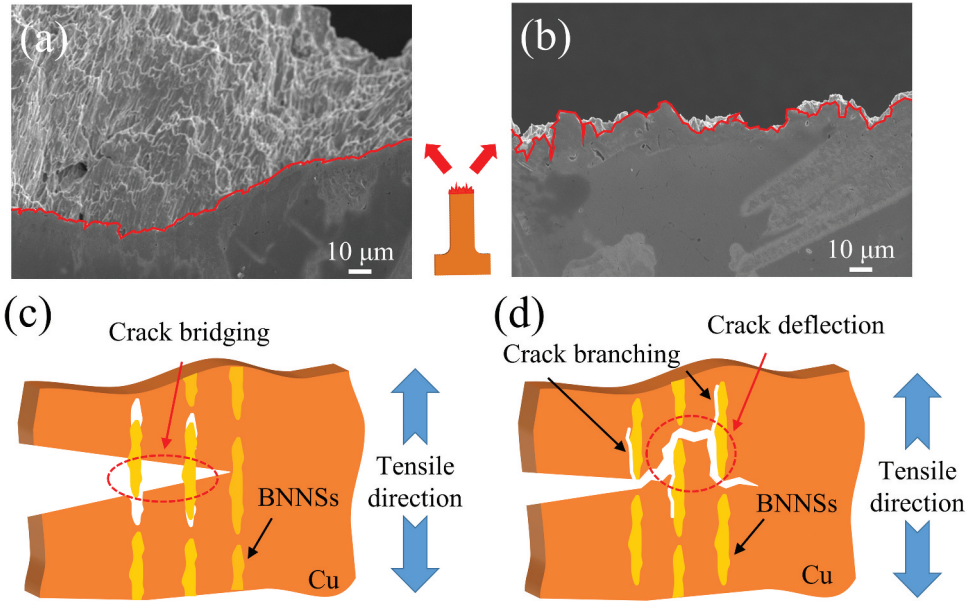
Figure 8. SEM images of the trace of crack of (a) P-Cu and (b) 0.3-CMC. Schematic of the toughening mechanisms: (c) Crack bridging; (d) Crack deflection and branching.

content was 0.3 vol%. The work of fracture (WOF) of BNNSs/Cu composites was measured by calculating the area under the stress-strain curve, which represents the ability of materials to absorb energy up to fracture under load [43]. The maximum WOF of 104.5 MJ/m^3 was obtained when the BNNSs content was 0.3 vol%, 73.9% more compared to P-Cu. These results suggest that the combination of strength and toughness have been achieve in this study.

Figure 7 shows the fracture surfaces of P-Cu and BNNSs/Cu composites with different BNNSs contents. A lot of large dimples were observed on the fracture surface of P-Cu, which is the typical feature of plastic feature (Figure 7a and b). In 0.3-CMC, the fracture surface was characterized by small dimples (Figure 7c). Notably, debonded BNNSs can be observed on the fracture surface, which suggests that BNNSs were pulled out during the tensile process (Figure 7d). As the BNNSs content further increases, the fracture surface gradually became flat and the amount of dimples declined (Figure 7e). Many BNNSs were exposed on the fracture surface (Figure 7f).

3.4 Discussion on toughening mechanisms

The composites exhibit higher toughness than pure Cu does. Figure 8a and b shows the crack trace images of P-Cu and 0.3-CMC. The crack trace of 0.3-CMC (Figure 8b) exhibited a more tortuous path than that of P-Cu (Figure 8a), which indicates the composites possess higher crack propagation resistance [44]. According to the above-mentioned fracture behaviors, the schematic drawing of the main toughening mechanisms of composites are shown in Figure 8c and d. These mechanisms are associated with the unique lamellar distribution of BNNSs [45–48]. First, the pulled-out BNNSs were observed (Figure 7d), demonstrating that crack bridging (as shown in Figure 8c) takes toughening effect in composites. The BNNSs connected two crack faces and served as bridges to transfer tractions between the two crack faces, enhancing the resistance of crack propagation and thus delayed the fracture. Second, due to the lamellar distribution of BNNSs, crack deflection and branching (as shown in Figure 8d) occurred as the crack came close to BNNSs, which dissipated greater energy and thus improved the resistance of crack propagation. When it encountered BNNSs, the crack was forced to move out of its initial propagation direction and then deflected to move along the meandering BNNSs/Cu interface. As a result, such deflection and branching processes caused a tortuous crack path (Figure 8b). Therefore, crack pass through the lamellar distribution zones of BNNSs by consuming more energy, leading to an increased toughness. In fact, the effect of above toughening mechanisms are influenced by the interfacial bonding strength between the BNNSs and Cu matrix [49]. In addition, grain refinement also accounts for the increased toughness in the composites, as the introduction of BNNSs can refine the Cu matrix [50,51].

3.5 The influences of BNNSs content on the strength

The tensile strength of the composites varies a little with the BNNSs contents. This is in a contrast with some reported results. For example, Yoo et al. [38] reported that the addition of 1.0 vol% and 2.5 vol% of BNNSs into Cu generates an increase of 7% and 48% in UTS, respectively. However, the study by Wang et al. [52] showed that the UTS was increased by 41% and 16% by adding 0.5 wt.% and 1.5 wt.% graphene into Cu, respectively. Their results show that the content of reinforcement has a big impact on the strength, which can be an increase or a decrease.

The marginal variation of strength of the composite is related to the interfacial bonding strength and agglomeration of BNNSs. There are several possible strengthening mechanisms for BNNSs/Cu composites [53–56], namely grain refinement, dislocation

strengthening, Orowan strengthening, and load transfer. The former two mechanisms are irrelevant to the interfacial bonding strength. Their contribution to the strength increases with the BNNSs content: more BNNSs can hinder the grain growth in the sintering process; more severe deformation is needed for the composite with higher BNNSs content, leading to higher dislocation density. However, they can only lead to a slight strength increase. Orowan strengthening and load transfer act only if the interfacial bonding strength is high enough. Otherwise, the debonding between BNNSs and Cu occurs prematurely, reducing the strengthening effect. The bonding between BNNSs and Cu is mainly diffusion bonding, which can be verified by the fact that neither voids nor interfacial reaction products existed (Figure 5) [57]. Such type of bonding has a moderate strength [41,42]. Thus, these two mechanisms may fail to fully act as a result of premature debonding between BNNSs and Cu [58–60]. This means that the contribution of these two mechanisms are also slight. Therefore, the improvement of strength with the addition of BNNSs is not significant. In addition, the strengthening effects of BNNSs may be offset by the weakening effects of their agglomeration, when excessive amount is introduced. This is because the fracture of composites would take place among the agglomerated nanosheets. This is evidenced by many BNNSs bonded to the Cu matrix in the fracture surface of 0.8-CMC (Figure 7f), in contrast to the debonded BNNSs in the fracture surface of 0.3-CMC (Figure 7d). As a result of weak bonding between agglomerated sheets, the fracture among them leads to the decreased tensile strength. Such phenomenon was also found in the Cu-based composites reinforced with graphene nanosheets [61] and Al-based composites reinforced with BNNSs [62]. As a result of moderate bonding strength and the effects of agglomeration, only minor change of strength with BNNSs content was noticed.

4. Conclusions

In summary, BNNSs/Cu composites with a bioinspired laminated structure were fabricated by ball milling and then SPS. With the increase of BNNSs content, both the tensile strength and the elongation increase initially and decrease later. The addition of 0.3 vol% of BNNSs improves the tensile strength from 187 MPa to 216 MPa and the elongation from 41% to 56%, respectively. The lamellar distribution of BNNSs leads to the crack bridging, deflection and branching during crack propagation. All these improved the resistance of crack propagation and thus contributed to their higher toughness compared with pure Cu. Furthermore, the moderate interfacial bonding strength and possible agglomeration of BNNSs may account for the minor change of strength with BNNSs content. This study regulates the properties of Cu-based matrix composites by using BNNSs, and shows the potential applications of BNNSs as the ideal reinforcement in Cu-based matrix composites.

CAS.

Disclosure statement

Funding

ORCID

Hua Li ⓘD http://orcid.org/0000-0002-8786-4295

References

[1] López M, Corredor D, Camurri C, et al. Performance and characterization of dispersion strengthened Cu–TiB2 composite for electrical use. Mater Charact. 2005;55(4–5):252–262. .

[2] Bai G, Wang L, Zhang Y, et al. Tailoring interface structure and enhancing thermal conductivity of Cu/diamond composites by alloying boron to the Cu matrix. Mater Charact. 2019;152:265–275.

[3] Akhtar F, Askari SJ, Shah KA, et al. Microstructure, mechanical properties, electrical conductivity and wear behavior of high volume TiC reinforced Cu-matrix composites. Mater Charact. 2009;60(4):327–336. .

[4] Li J, Wang X, Qiao Y, et al. High thermal conductivity through interfacial layer optimization in diamond particles dispersed Zr-alloyed Cu matrix composites. Scr Mater. 2015;109:72–75.

[5] Li C, Xie Y, Zhou D, et al. A novel way for fabricating ultrafine grained Cu-4.5 vol% Al_2O_3 composite with high strength and electrical conductivity. Mater Charact. 2019;155:109775.

[6] Yuan Y, Gan X, Lai Y, et al. Microstructure and properties of graphite/copper composites fabricated with Cu-Ni double-layer coated graphite powders. Compos Interfaces. 2019;27 (5):449–463. .

[7] Liao Q, Wei W, Zuo H, et al. Interfacial bonding enhancement and properties improvement of carbon/copper composites based on nickel doping. Compos Interfaces. 2020;2:1–13.

[8] Salvo C, Mangalaraja RV, Udayabashkar R, et al. Enhanced mechanical and electrical properties of novel graphene reinforced copper matrix composites. J Alloys Compd. 2019;777:309–316.

[9] Gao X, Yue H, Guo E, et al. Mechanical properties and thermal conductivity of graphene reinforced copper matrix composites. Powder Technol. 2016;301:601–607.

[10] Çelikyürek İ, Nö K, Ölçer T, et al. Microstructure, properties and wear behaviors of $(Ni_3Al)_p$ reinforced Cu matrix composites. J Mater Sci Technol. 2011;27(10):937–943. .

[11] Meyers MA, Chen PY, Lin AYM, et al. Biological materials: structure and mechanical properties. Prog Mater Sci. 2008;53(1):1–206.

[12] Dunlop JWC, Fratzl P. Biological Composites. Annu Rev Mater Res. 2010;40(1):1–24.

[13] George J, Ishida H. A review on the very high nanofiller-content nanocomposites: their preparation methods and properties with high aspect ratio fillers. Prog Polym Sci. 2018;86:1–39.

[14] Mayer G. Rigid biological systems as models for synthetic composites. Science. 2005;310 (5751):1144–1147.

[15] Ritchie RO. The conflicts between strength and toughness. Nat Mater. 2011;10(11):817–822.

[16] Gao H, Ji B, Jager IL, et al. Materials become insensitive to flaws at nanoscale: lessons from nature. Proc Natl Acad Sci U S A. 2003;100(10):5597–5600. .

[17] Ji B, Gao H. Mechanical properties of nanostructure of biological materials. J Mech Phys Solids. 2004;52(9):1963–1990.

[18] Espinosa HD, Juster AL, Latourte FJ, et al. Tablet-level origin of toughening in abalone shells and translation to synthetic composite materials. Nat Commun. 2011;2(1):173. .

[19] Clegg WJ, Howard SJ, Lee W, et al. Interfacial cracking in ceramic laminates. Compos Interfaces. 2012;2(5):337–349. .

[20] Li J, Zhao M, Jin L, et al. Simultaneously improving strength and ductility through laminate structure design in Mg–8.0Gd–3.0Y-0.5Zr alloys. J Mater Sci Technol. 2021;71:195–200.

[21] Li YH, Housten W, Zhao YM, et al. Cu/single-walled carbon nanotube laminate composites fabricated by cold rolling and annealing. Nanotechnology. 2007;18:20.

[22] Kang TJ, Yoon JW, Kim DI, et al. Sandwich-Type laminated nanocomposites developed by selective dip-coating of carbon nanotubes. Adv Mater. 2007;19(3):427–432. .

[23] Jiang L, Li Z, Fan G, et al. Strong and ductile carbon nanotube/aluminum bulk nanolaminated composites with two-dimensional alignment of carbon nanotubes. Scr Mater. 2012;66 (6):331–334. .

[24] Tjong SC. Recent progress in the development and properties of novel metal matrix nanocomposites reinforced with carbon nanotubes and graphene nanosheets. Mater Sci Eng R Rep. 2013;74(10):281–350.

[25] Dorri Moghadam A, Omrani E, Menezes PL, et al. Mechanical and tribological properties of self-lubricating metal matrix nanocomposites reinforced by carbon nanotubes (CNTs) and graphene - A review. Compos B. 2015;77:402–420.

[26] Zhao Q, Gan X, Lei Q, et al. Enhanced the strength and ductility of the partially unzipped carbon nanotubes reinforced CuCr matrix composites via optimization of the interface structure. Compos Interfaces. 2020;27(10):893–903. .

[27] Song Z, Hu X, Xiang Y, et al. Enhanced mechanical properties of CNTs/Mg biomimetic laminated composites. Mater Sci Eng A. 2021;802:140632.

[28] Wang J, Li Z, Fan G, et al. Reinforcement with graphene nanosheets in aluminum matrix composites. Scr Mater. 2012;66(8):594–597. .

[29] Ouyang T, Chen Y, Xie Y, et al. Thermal transport in hexagonal boron nitride nanoribbons. Nanotechnology. 2010;21(24):245701. .

[30] Wei X, Wang MS, Bando Y, et al. Tensile tests on individual multi-walled boron nitride nanotubes. Adv Mater. 2010;22(43):4895–4899. .

[31] Suryavanshi AP, Yu M-F, Wen J, et al. Elastic modulus and resonance behavior of boron nitride nanotubes. Appl Phys Lett. 2004;84(14):2527–2529. .

[32] Falin A, Cai Q, Santos EJG, et al. Mechanical properties of atomically thin boron nitride and the role of interlayer interactions. Nat Commun. 2017;8(1):15815. .

[33] Jo I, Pettes MT, Kim J, et al. Thermal conductivity and phonon transport in suspended few-layer hexagonal boron nitride. Nano Lett. 2013;13(2):550–554. .

[34] Golberg D, Bando Y, Huang Y, et al. Boron nitride nanotubes and nanosheets. ACS Nano. 2010;4(6):2979–2993. .

[35] Zhu YC, Bando Y, Xue DF, et al. Insulating tubular BN sheathing on semiconducting nanowires. J Am Chem Soc. 2003;125(47):14226–14227. .

[36] Wang T, Wei C, Yan L, et al. Thermally conductive, mechanically strong dielectric film made from aramid nanofiber and edge-hydroxylated boron nitride nanosheet for thermal management applications. Compos Interfaces. 2020;8:1–14.

[37] Pawlak Z, Kaldonski T, Pai R, et al. A comparative study on the tribological behaviour of hexagonal boron nitride (h-BN) as lubricating micro-particles-An additive in porous sliding bearings for a car clutch. Wear. 2009;267(5–8):1198–1202. .

[38] Yoo SC, Kim J, Lee W, et al. Enhanced mechanical properties of boron nitride nanosheet/copper nanocomposites via a molecular-level mixing process. Compos B. 2020;195:108088.

[39] Veillère A, Heintz JM, Chandra N, et al. Influence of the interface structure on the thermo-mechanical properties of Cu-X (X=Cr or B)/carbon fiber composites. Mater Res Bull. 2012;47(2):375–380. .

[40] Füllgrabe M, Ittermann B, Stöckmann HJ, et al. Diffusion parameters of B in Cu determined by β-radiation-detected NMR. Phys Rev B. 2001;64(22):22. .

[41] Liu BX, Huang LJ, Geng L, et al. Fabrication and superior ductility of laminated Ti-TiBw/Ti composites by diffusion welding. J Alloys Compd. 2014;602:187–192.

[42] Liu BX, Huang LJ, Kaveendran B, et al. Tensile and bending behaviors and characteristics of laminated Ti-(TiBw/Ti) composites with different interface status. Compos B. 2017;108:377–385.

[43] Paramsothy M, Hassan SF, Srikanth N, et al. Enhancing tensile/compressive response of magnesium alloy AZ31 by integrating with Al_2O_3 nanoparticles. Mater Sci Eng A. 2009;527(1–2):162–168. .

[44] Shan Y, Pu B, Liu E, et al. In-situ synthesis of CNTs@Al_2O_3 wrapped structure in aluminum matrix composites with balanced strength and toughness. Mater Sci Eng A. 2020;797:140058.

[45] Zhang X, Shi C, Liu E, et al. Effect of interface structure on the mechanical properties of graphene nanosheets reinforced copper matrix composites. ACS Appl Mater Interfaces. 2018;10(43):37586–37601. .

[46] Feng S, Guo Q, Li Z, et al. Strengthening and toughening mechanisms in graphene-Al nanolaminated composite micro-pillars. Acta Mater. 2017;125:98–108.

[47] Li Z, Guo Q, Li Z, et al. Enhanced mechanical properties of graphene (reduced graphene oxide)/aluminum composites with a bioinspired nanolaminated structure. Nano Lett. 2015;15(12):8077–8083. .

[48] Xiong DB, Cao M, Guo Q, et al. Graphene-and-copper artificial nacre fabricated by a preform impregnation process: bioinspired strategy for strengthening-toughening of metal matrix composite. ACS Nano. 2015;9(7):6934–6943. .

[49] Zhou J, Yuan M, Li Z, et al. A great improvement of tensile properties of Cf/AZ91D composite through grafting CNTs onto the surface of the carbon fibers. Mater Sci Eng A. 2019;762:138061.

[50] Noronha SJ, Farkas D. Effect of dislocation blocking on fracture behavior of Al and α-Fe: a multiscale study. Mater Sci Eng A. 2004;365(1–2):156–165.

[51] Cui C, Gao Y, Wei S, et al. Microstructure and high temperature deformation behavior of the Mo-ZrO_2 alloys. J Alloys Compd. 2017;716:321–329.

[52] Wang J, Guo LN, Lin WM, et al. The effects of graphene content on the corrosion resistance, and electrical, thermal and mechanical properties of graphene/copper composites. New Carbon Mater. 2019;34(2):161–169. .

[53] Shin SE, Choi HJ, Shin JH, et al. Strengthening behavior of few-layered graphene/aluminum composites. Carbon. 2015;82:143–151.

[54] Mu XN, Zhang HM, Cai HN, et al. Microstructure evolution and superior tensile properties of low content graphene nanoplatelets reinforced pure Ti matrix composites. Mater Sci Eng A. 2017;687:164–174.

[55] Park JG, Keum DH, Lee YH. Strengthening mechanisms in carbon nanotube-reinforced aluminum composites. Carbon. 2015;95:690–698.

[56] Zhang Z, Chen D. Consideration of Orowan strengthening effect in particulate-reinforced metal matrix nanocomposites: a model for predicting their yield strength. Scr Mater. 2006;54(7):1321–1326.

[57] Chen Z, Tan Z, Ji G, et al. Effect of interface evolution on thermal conductivity of vacuum hot pressed SiC/Al composites. Adv Eng Mater. 2015;17(7):1076–1084. .

[58] Chu K, Wang F, Li YB, et al. Interface and mechanical/thermal properties of graphene/copper composite with Mo_2C nanoparticles grown on graphene. Compos Part A Appl Sci Manuf. 2018;109:267–279.

[59] Liu X, Liu E, Li J, et al. Investigation of the evolution and strengthening effect of aluminum carbide for in-situ preparation of carbon nanosheets/aluminum composites. Mater Sci Eng A. 2019;764:138139.

[60] Hwang J, Yoon T, Jin SH, et al. Enhanced mechanical properties of graphene/copper nanocomposites using a molecular-level mixing process. Adv Mater. 2013;25 (46):6724–6729. .

[61] Yue H, Yao L, Gao X, et al. Effect of ball-milling and graphene contents on the mechanical properties and fracture mechanisms of graphene nanosheets reinforced copper matrix composites. J Alloys Compd. 2017;691:755–762.

[62] Yusupov KU, Corthay S, Bondarev AV, et al. Spark plasma sintered Al-based composites reinforced with BN nanosheets exfoliated under ball milling in ethylene glycol. Mater Sci Eng A. 2019;745:74–81.